

# Chemistry of the Aqueous Phase of Ordinary Portland Cement Pastes at Early Reaction Times

Anthony L. Kelzenberg,<sup>†</sup> Sharon L. Tracy,<sup>\*,†</sup> Bruce J. Christiansen,<sup>\*,†</sup> Jeffrey J. Thomas,<sup>\*,‡</sup>  
 Matthew E. Clarage,<sup>§</sup> Simon Hodson,<sup>¶</sup> and Hamlin M. Jennings<sup>\*,†,‡</sup>

Department of Materials Science and Engineering, Northwestern University, Evanston, Illinois 60208;  
 National Cement and Ceramics Laboratory (NCCL), Wilmette, Illinois 60091; Department of Civil Engineering,  
 Northwestern University, Evanston, Illinois 60209; and E. Khashoggi Industries (EKI),  
 Santa Barbara, California 93109

The chemistry of the aqueous phase of ordinary portland cement paste at early ages (<2 h) has been analyzed in terms of the concentrations of the elemental components in the pore fluid. The concentrations of calcium, sulfur, aluminum, and silicon are rationalized by plotting the data on “phase diagrams.” To simplify the analysis, the portland cement system is described using two subsystems: (i) CaO–Al<sub>2</sub>O<sub>3</sub>–CaSO<sub>4</sub>–H<sub>2</sub>O, modified by the presence of sodium and potassium, and (ii) CaO–SiO<sub>2</sub>–H<sub>2</sub>O. During the first 10 min of hydration, the calcium, sulfur, and aluminum concentrations all decrease, roughly in proportion, which suggests a precipitation process, a conversion of calcium sulfate hemihydrate to gypsum, and the initial formation of ettringite. The CaO–Al<sub>2</sub>O<sub>3</sub>–CaSO<sub>4</sub>–H<sub>2</sub>O subsystem seems to move from a phase assemblage of gypsum, Al<sub>2</sub>O<sub>3</sub>·3H<sub>2</sub>O, and ettringite to an assemblage of gypsum, calcium hydroxide, and ettringite during the first 15–30 min after the water and the cement are mixed. The silicate equilibrium is approached more slowly. The intensity of mixing has relatively little effect on the concentrations beyond the first few minutes.

## I. Introduction

THE microstructure and materials science of cements have been the subject of study for more than 100 years, yet some of the basic tools of materials science are not yet available. In particular, progress in understanding the chemistry of these systems has been relatively slow. Although the phase diagrams relevant to cementitious systems are available, there is not yet widespread agreement as to whether phase diagrams can be applied to hydrating cement pastes at all, particularly at early ages, when the system is undergoing relatively rapid changes. However, recent research indicates that phase diagrams are indeed a valuable way to represent cement systems. For example, Damidot and Glasser at the University of Aberdeen<sup>1,2</sup> recently published several quaternary phase diagrams of the CaO–Al<sub>2</sub>O<sub>3</sub>–CaSO<sub>4</sub>–H<sub>2</sub>O system.

One of the difficulties with using phase diagrams for cement

systems is the number of components that must be represented. Portland cement is at least a six-component system (CaO, SiO<sub>2</sub>, H<sub>2</sub>O, Al<sub>2</sub>O<sub>3</sub>, CaSO<sub>4</sub>, and alkalis), and representation of the phase relationships on a single diagram is impractical. Another difficulty is that the composition of the aqueous phase changes rapidly during the early period of reaction, making it difficult to obtain accurate data.

A basic requirement must be satisfied before cement systems at early reaction times can be usefully represented using phase diagrams. First, the system must be in an equilibrium or pseudo-equilibrium state. By a pseudo-equilibrium state, we mean that the concentrations of components in the aqueous phase are controlled by the solubility products of the solids, and these concentrations are approached rapidly compared to changes that occur because of dissolution and precipitation. This definition is frequently used in chemical engineering to analyze reacting systems. Thus, pseudo-equilibrium implies that the Gibbs phase rule is obeyed and concentrations are near a solidus line, as has been argued for the pure tricalcium silicate system;<sup>3</sup> this line is a state function, i.e., independent of previous history. Perhaps some insight into the issue of equilibrium can be drawn from Le Chatelier’s law, which can be interpreted as follows. If a system is in equilibrium, it resists changes in concentration (as well as other changes) that may be imposed on it. In the case of equilibrium between the aqueous phase and cement, equilibrium is demonstrated by maintaining a position on the appropriate phase boundary even though the concentration of a component is changing. Finally, it would be very convenient if the system could be divided into two or more subsystems for the purpose of analysis. This aspect allows a multicomponent system to be simplified for the purpose of graphical representation.

The concentrations of components in the aqueous phase of portland cement pastes have been measured by several researchers<sup>4–7</sup> for times between the first few minutes and 24 h after mixing. These studies show that, for times of 2–12 h, there are relatively small changes in the concentrations of calcium, potassium, sodium, and alkalis, which suggests that some type of equilibrium is established or that the rates of continued dissolution of the cement phases and the precipitation of cement hydration products are equal.<sup>8</sup> Between 12 and 16 h after mixing, the concentrations of calcium and sulfur decrease sharply, and the solution becomes essentially one of alkali hydroxides. This decrease corresponds to the renewed hydration of the calcium aluminates phases.<sup>8,9</sup>

Very little information has been published on the composition of the aqueous phase at times much earlier than 2 h. In particular, there is a lack of data that includes all components of these systems because silicon and aluminum are typically present in the aqueous phase only in micromolar concentrations, and only recently has modern instrumentation allowed routine analysis. Double<sup>4</sup> reported some data for this period, but the water:cement (w:c) ratios were high (w:c = 2). The concentrations of calcium and sulfur fell rapidly during the first

P. Brown—contributing editor

Manuscript No. 192475. Received March 25, 1996; approved March 20, 1997.  
 Supported by the NCCL and the National Science Foundation (NSF) Science and Technology Center for Advanced Cement Based Materials (Award No. DMR 9120002).

<sup>†</sup>Member, American Ceramic Society.

<sup>‡</sup>Department of Materials Science and Engineering, Northwestern University.

<sup>§</sup>Department of Civil Engineering, Northwestern University.

<sup>¶</sup>NCCL.

<sup>¶</sup>EKI.

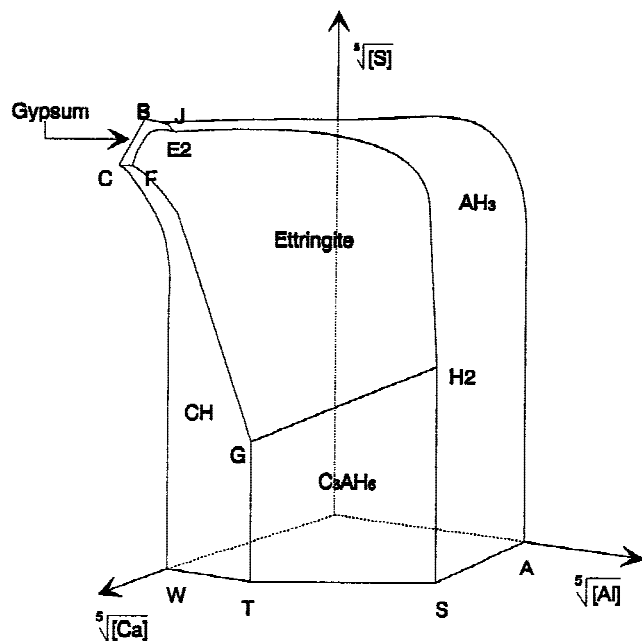


Fig. 1. Reproduction of the phase diagram calculated by Damidot and Glasser<sup>2</sup> for the CaO–CaSO<sub>4</sub>–Al<sub>2</sub>O<sub>3</sub>–H<sub>2</sub>O system, modified with 0.178M of potassium. The axis units are the concentrations of sulfur, calcium, and aluminum, plotted as fifth roots of the molarity.

10 min, which was attributed to the precipitation of sulphoaluminate hydrates.<sup>4</sup> As summarized by Scrivener,<sup>9</sup> this hypothesis is consistent with transmission electron microscopy (TEM) studies that demonstrate the early formation (within 10 min of hydration) of an amorphous colloidal layer on portland cement grains that contains significant amounts of calcium and sulfate, as well as alumina and silica.

This paper reports results that are designed to make a first-approximation attempt at formulating phase diagrams for the portland cement system during the early stages of reaction (the first 2 h after the cement and water are mixed). The results from pastes made with two typical w:c values (0.4 and 0.7) are discussed, as well as the influence of mixing intensity.

### (1) The CaO–Al<sub>2</sub>O<sub>3</sub>–CaSO<sub>4</sub>–H<sub>2</sub>O System (The Aluminate System): Previous Results and Models

The phase relationships in this system have been studied for many years, starting with the experimental work of Jones,<sup>10–12</sup> D'Ans and Eick,<sup>13</sup> and, more recently, Brown,<sup>14</sup> and Damidot and Glasser.<sup>1,2</sup> This system has particular relevance to the early stages of cement hydration. When water and cement are combined, there is initially a combination of exothermic wetting and the early stage reactions, which result in a gelatinous coating and rods of the AFT phase.<sup>9</sup> The primary AFT phase is ettringite (3CaO·Al<sub>2</sub>O<sub>3</sub>·3CaSO<sub>4</sub>·32H<sub>2</sub>O), which is a stable phase in the presence of excess calcium sulfate that forms

Table I. Solubility Data Used in Computations

Mineral	log <i>K</i> <sub>sp</sub>
C <sub>3</sub> AH <sub>6</sub> <sup>†</sup>	78.66
C <sub>3</sub> AH <sub>6</sub> <sup>‡</sup>	80.35
Monosulphoaluminate	71.36
AH <sub>3</sub> (gibbsite)	7.228
Gypsum (C <sub>2</sub> H <sub>2</sub> )	–4.60
CH (portlandite)	22.815
Ettringite	55.223
Syngenite	–7.45
Pentasalt	–29.3

<sup>†</sup>Both values are reported in the database used.<sup>17</sup>

Table II. Chemical Composition of Cement V (Type II) and Cement C (Type I)

Component	Composition (wt%)	
	Cement V	Cement C
By component		
SiO <sub>2</sub>	20.9	20.8
Al <sub>2</sub> O <sub>3</sub>	4.5	4.6
Fe <sub>2</sub> O <sub>3</sub>	3.4	2.6
CaO	62.4	63.2
MgO	4.7	4.2
SO <sub>3</sub>	2.6	2.7
Loss on ignition	1.3	0.9
By cement compound		
C <sub>3</sub> S	53	54
C <sub>4</sub> AF	10	8
C <sub>3</sub> A	6	9
C <sub>2</sub> S	20	19
Alkalis (Na <sub>2</sub> O equiv.)	0.33	0.49

during the early hydration of most portland cements. This AFT phase covers much of the surface of the cement grains within the first 10–15 min; however, it is unclear whether the unreacted aluminates are thermodynamically isolated from the aqueous phase, as has been suggested for the silicates.<sup>3</sup> If so, these products control the concentrations of the aqueous species. It is also uncertain what role the AFT phase has in the induction period. This paper examines the thermodynamic solubilities of the aluminate products as if they are the only products formed and compares them with experimental pore solution concentrations obtained from portland cement pastes.

Damidot and Glasser<sup>1,2</sup> studied the equilibria in the CaO–Al<sub>2</sub>O<sub>3</sub>–CaSO<sub>4</sub>–H<sub>2</sub>O system by systematically computing the composition of the aqueous phase that is in equilibrium with various assemblages of solid phases. Two-dimensional slices of the three-dimensional space were computed and then combined to construct the complete diagram. Subsequently, the influence of Na<sub>2</sub>O and K<sub>2</sub>O at two fixed concentrations was investigated to study the effect of alkalis on the equilibria. Their phase diagram for CaO–Al<sub>2</sub>O<sub>3</sub>–CaSO<sub>4</sub>–H<sub>2</sub>O, modified with 0.178M of potassium, is reproduced in Fig. 1. The concentrations are plotted along the axes as fifth roots of their molarity, following the “nth root” method developed by Brown.<sup>14</sup>

In the work reported here, thermodynamic models and relevant databases suitable for cement systems<sup>15–17</sup> were used to compute the influence of experimentally determined concentrations of sodium and potassium in the pore fluids of portland cement on the theoretical aluminate system. Theoretical results computed without the silicates were then compared with the experimental results. If the system behaved as if it was in equilibrium, the relevant phase assemblages could then be determined. It should be emphasized that alkalis must be included in models that predict aqueous phase compositions because of their effect on the concentrations of the other ions.

The values for the solubility products used in the models were critical to predicting which phases are stable. Data in the literature are sometimes incomplete or conflicting. For instance, in the database of the cement compounds used here,<sup>17</sup> two log *K*<sub>sp</sub> values for C<sub>3</sub>AH<sub>6</sub><sup>††</sup> are listed because the correct value has not yet been established. The best that can be done is to model the data using both values and note which value was used for any resulting predictions. Table I lists the *K*<sub>sp</sub> values used in our computations.

### (2) Equilibria in the CaO–SiO<sub>2</sub>–H<sub>2</sub>O System

Solubility relationships in this system have been studied both under equilibrium conditions (e.g., Flint and Wells<sup>18</sup> and Fujii

<sup>††</sup>Cement chemistry notation will be used here for compounds formed in cement paste. (C = CaO, S = SiO<sub>2</sub>, A = Al<sub>2</sub>O<sub>3</sub>, S̄ = SO<sub>3</sub>, and H = H<sub>2</sub>O.)

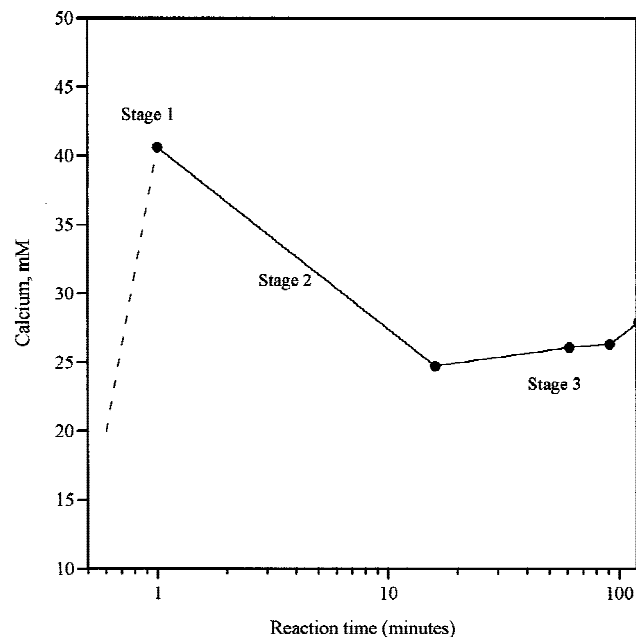


**Fig. 2.** Plot of calcium concentration in the aqueous phase versus time immediately after mixing; the reaction is divided into three stages, as shown. The concentrations of sulfur and aluminum follow similar paths.

and Kondo<sup>19</sup>) and from the standpoint of time-dependent variations during the hydration of tricalcium silicate ( $C_3S$ ).<sup>20-23</sup> Jennings<sup>3</sup> demonstrated that the concentrations of  $CaO$  and  $SiO_2$  from many different studies fall on two general curves that represent the solubilities of stable and metastable phases of the C-S-H gel. The system  $CaO-SiO_2-H_2O-Na_2O$  was studied by Brown,<sup>24</sup> who constructed a quaternary phase diagram using the available data, and the composition of the aqueous phase during the hydration of  $C_3S$  was modeled by Brown and Shi.<sup>25</sup> The present study analyzes the aqueous phase chemistry in terms of the phase diagrams for the pure  $CaO-SiO_2-H_2O$  system, both in the presence and absence of alkalis.

## II. Experimental Procedure

The cement pastes used in this study were made by mixing deionized water with portland cement at room temperature, using a w:c ratio of either 0.4 or 0.7. Two portland cements were used, and the chemical compositions of these cements, hereafter called cements V and C, are given in Table II. The principal difference between cement V and cement C is the concentration of alkalis.

Two mixers with different mixing energies were used to mix the pastes. One mixer was a standard Hobart mixer (Model N-50, Hobart Manufacturing Co., Troy, OH) set at speed 1, and the other was a high-energy mixer (HEM), which had an internal blade that rotated at 500 rpm. The HEM is a propeller-driven counter-current tube mixer that has been described in a U.S. patent.<sup>26</sup> Because of fundamentally different designs, the shear rates of these two mixers cannot be directly compared; however, the HEM imparts much higher shear to the paste than does the Hobart mixer.

To study the aqueous phase after short reaction times ( $<10$  min), the samples were mixed for times of 1 and 3 min. The 1-min mix procedure consisted of 30 s during which the cement was fed into the mix chamber, followed by 30 s of additional mixing. Pore solution samples for the 1-min mix were extracted from the pastes 1, 5, and 9 min after the start of mixing. This extraction was accomplished by vacuum filtering under a  $CO_2$ -free nitrogen atmosphere. Pore solution samples for the 3-min mix procedure were taken 3 and 8 min after mutual contact of reactants. For longer reaction times (up to 2 h), paste samples were mixed for either 1 or 5 min and then vacuum-filtered 15, 30, 45, 60, 90, and 120 min after the start of mixing. After filtration, the aqueous solutions were analyzed by using inductively coupled plasma-atomic emission spectroscopy (ICP-AES) to determine millimolar concentrations of calcium, sulfur, sodium, and potassium, and micromolar concentrations of aluminum and silicon.

## III. Results and Discussion

The experimental results are subdivided and discussed in two separate groupings: (i) the aluminate sulfates (the  $CaO-Al_2O_3-SO_3-H_2O$  system) and (ii) the silicates (the  $CaO-SiO_2-H_2O$  system). In this paper, elemental concentrations are used as the components of the systems and to describe ionic con-

**Table III.** Elemental Concentrations during the First 10 min after Initial Mixing<sup>†</sup>

Time (min)	Cement V			Cement C		
	[Ca] (mM)	[Al] (mM)	[S] (mM)	[Ca] (mM)	[Al] (mM)	[S] (mM)
	High-energy mixer, w:c = 0.4, mix time = 1 min					
2	37.1	109.1	49.8	30.9	94.3	72.3
6	26.6	91.9	36.1	19.2	75.4	61.1
10	23.1	84.7	30.8	18.5	74.5	58.1
	Hobart mixer, w:c = 0.4, mix time = 1 min					
2	29.9	101.8	35.0	10.7	66.6	24.4
6	25.6	99.3	31.8	14.1	73.3	45.3
10	21.9	87.2	24.0	11.8	66.9	40.6
	Hobart mixer, w:c = 0.4, mix time = 3 min					
3	34.4	112.3	41.3	24.4	99.7	66.4
8	25.2	93.3	28.4	24.6	98.3	77.1
	High-energy mixer, w:c = 0.7, mix time = 1 min					
2	32.7	119.9	26.6	40.9	130.4	61.6
6	44.9	135.5	35.1	22.2	95.2	41.6
10	35.5	121.0	27.3	17.0	83.2	31.5
	Hobart mixer, w:c = 0.7, mix time = 1 min					
2	50.2	136.2	44.5	33.7	119.4	50.8
6	33.7	110.4	26.8	23.5	96.3	41.8
10	31.2	102.9	20.8	18.1	84.9	33.7
	Hobart mixer, w:c = 0.7, mix time = 3 min					
3	46.2	129.4	43.5	32.4	114.7	56.2
8	49.8	135.7	47.9	36.2	119.5	63.7

<sup>†</sup>Each data point represents an average value from one to four runs.

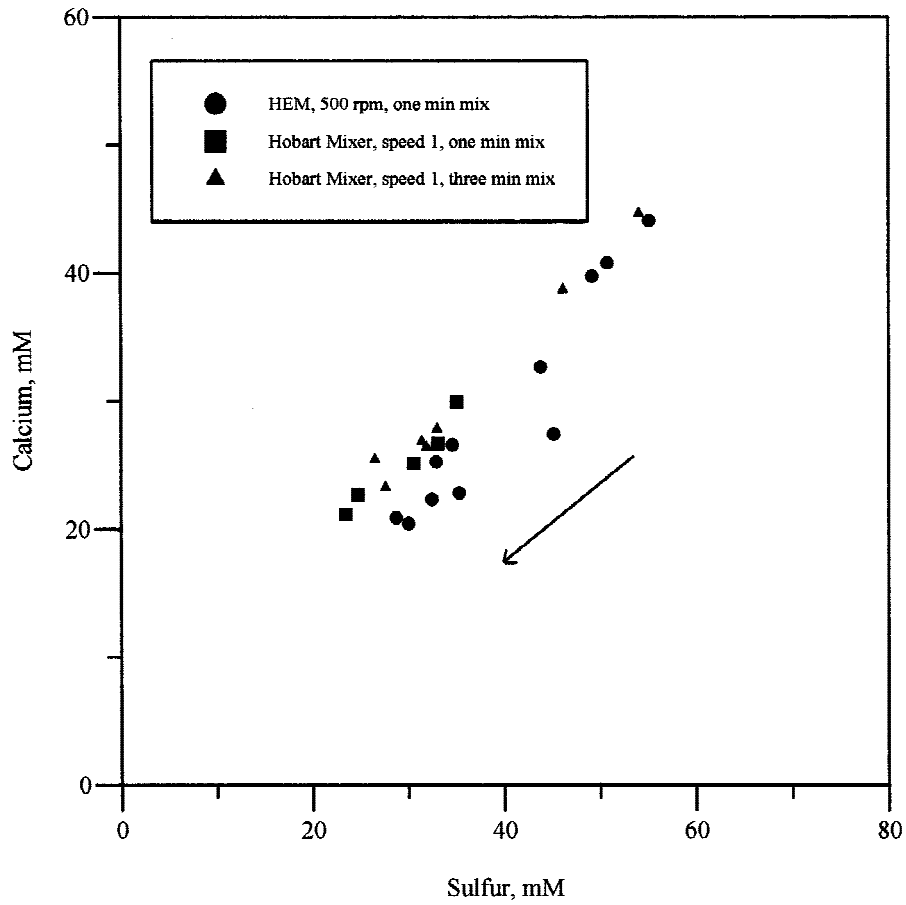


Fig. 3. Plot of calcium concentration versus sulfur concentration for cement V pastes, at w:c = 0.4, for the first 10 min after mixing.

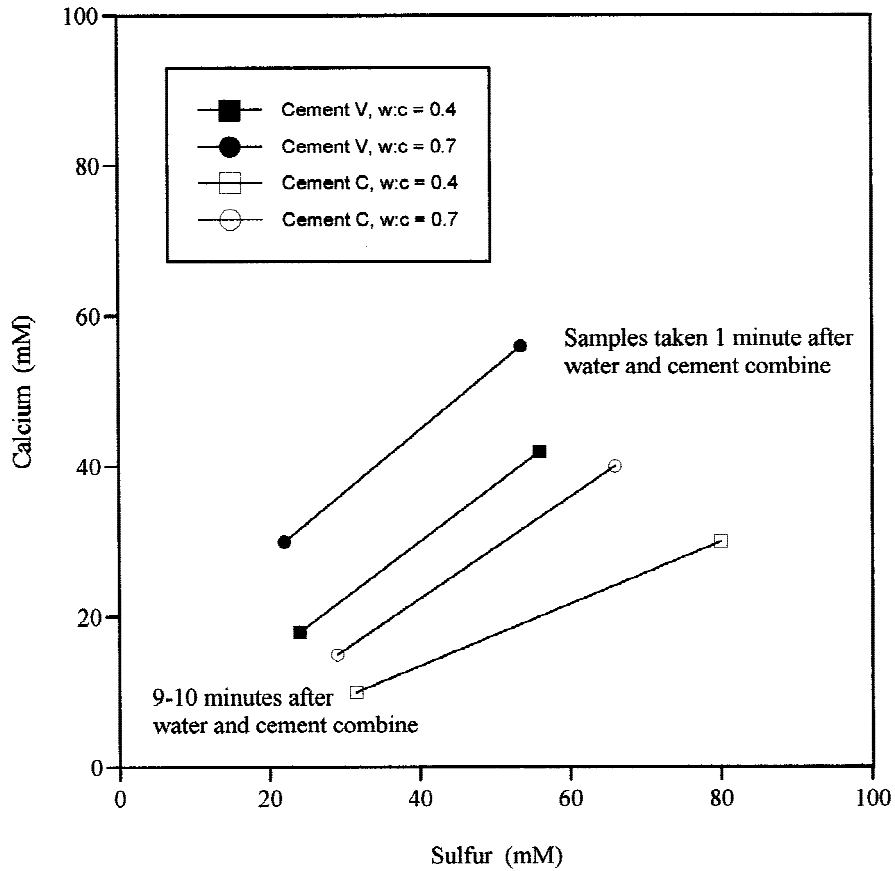


Fig. 4. Straight-line fits to the data for calcium concentration versus sulfur concentration for all the experimental conditions, for the first 10 min after mixing.

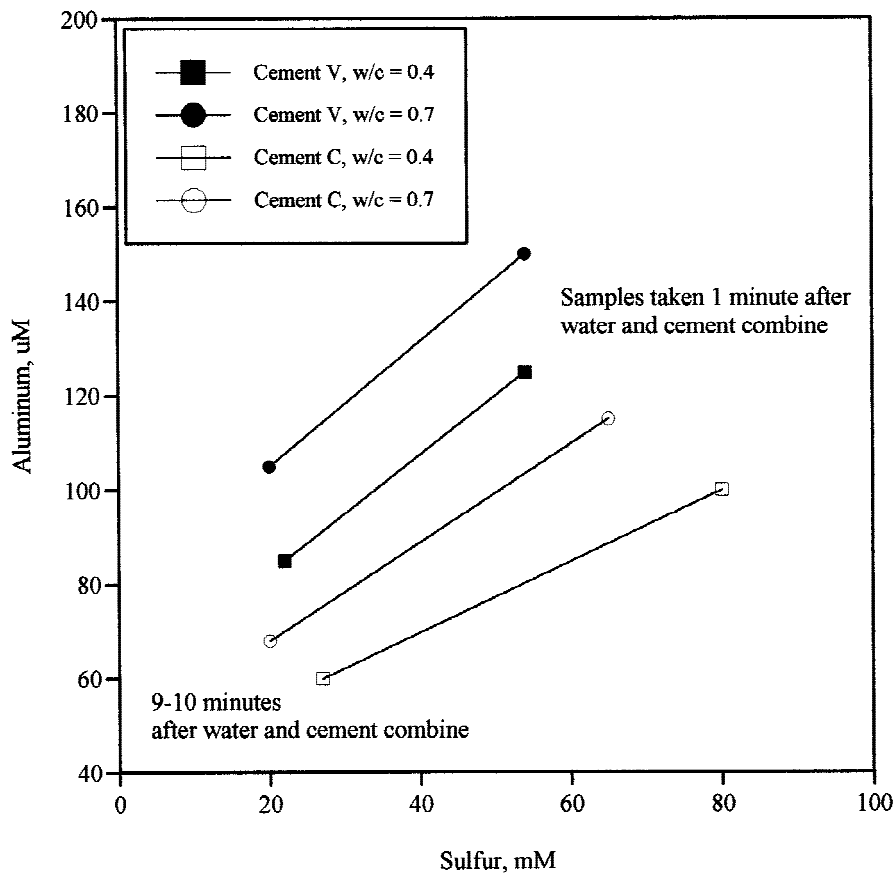


Fig. 5. Straight-line fits to the data for aluminum concentration versus sulfur concentration for all the experimental conditions, for the first 10 min after mixing.

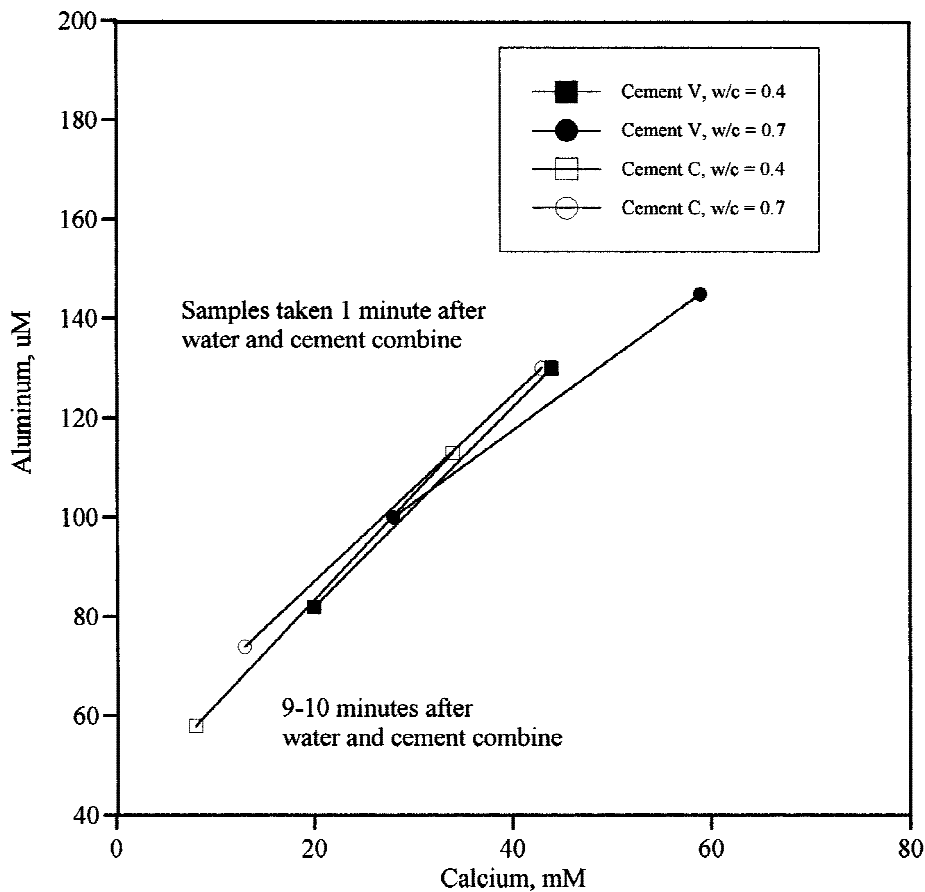


Fig. 6. Straight-line fits to the data for aluminum concentration versus calcium concentration for all the experimental conditions, for the first 10 min after mixing.



centrations of the aqueous ions because these variables are what were actually measured experimentally. This process also conveniently avoids any implication as to which species are present. However, this is not to say that there is any doubt that, for example, the sulfur is mainly present as  $\text{SO}_4^{2-}$ .

The portland cement system is a six-component system including alkalis (if  $\text{Na}_2\text{O}$  and  $\text{K}_2\text{O}$  are regarded as being equivalent in their behavior); thus, for each of these groups, additional axes that represent the other components are present but cannot be shown in two- or even three-dimensional space. In other words, the phase diagrams (or possibly pseudo-phase diagrams) shown are three-dimensional (silicate) or four-dimensional (aluminate) slices through at least a six-dimensional space. Although these subsystems are represented on separate diagrams, the aluminates and silicates are coupled and are not independently varying systems. The results of this paper support earlier assumptions that the portland cement system can be analyzed as separate subsystems within a six-dimensional space. At the very least, this paper demonstrates that concentrations of components in the aqueous phase obey reasonably well-defined patterns and rules.

### (I) Aluminate Sulfates: The $\text{CaO-Al}_2\text{O}_3\text{-SO}_3\text{-H}_2\text{O}$ System

(A) *The Three Stages of Early Reaction:* As will be shown below, the concentrations of calcium, sulfur, and aluminum in solution seem to be related. On the basis of these concentrations, the first few hours of reaction can be divided into three stages (see Fig. 2), as has been previously observed (e.g., see Double<sup>4</sup> and Lawrence<sup>6</sup>). Stage 1 (<1 min after water and cement come into contact) is a period of very rapid increase in the concentration of calcium from the dissolution of  $\text{C}_3\text{S}$ ,  $\text{C}_3\text{A}$ , and calcium sulfate. It should be noted that although all the calcium sulfate is added to the cement clinker in the form of gypsum ( $\text{CSH}_2$ ), dehydration during milling converts some of the gypsum to the more-soluble hemihydrate ( $\text{CSH}_{0.5}$ ). Stage 2 (1–15 min after water and cement come in contact) is a time during which the concentrations of calcium, sulfur, and aluminum all decrease. Stage 3 (16–120 min or more after water and cement come into contact) is a period during which the concentrations of the components in the aqueous phase remain relatively constant.

The above-mentioned stages are a general result, basically independent of the mixing time and type of mixer used. In other words, immediately after the water and cement are mixed, the reaction progresses according to a clock which starts when cement and water are first brought into contact. Mixing a cement paste for 1 min leaves the aqueous phase with elevated amounts of calcium, aluminum, and sulfur (near the end of Stage 1). These elements then precipitate within 15 min, during Stage 2. If a cement paste is mixed for 3 min and the aqueous phase is analyzed 12 min later, the concentrations are similar to those of a 1-min mix after 14 additional minutes (i.e., the reaction path is not greatly altered by mixing). Thus, early reaction products are chemically similar for all cement pastes, independent of mixing time.

(B) *Stages 1 and 2: The First 10 Min of Reaction:* The data taken during the first 10 min after the start of mixing for cement pastes made with cements V or C and having a w:c ratio of 0.4 or 0.7 exhibit several trends. The concentrations of calcium, aluminum, and sulfur always decrease from their highest value immediately after mixing to their lowest value (at ~10 min), indicating the approximate end of Stage 2 (see Table III). This initial decrease in concentration suggests that products precipitate even before the end of mixing, which is consistent with the general observation that the reaction path is not greatly altered by mixing. The plot of calcium concentration versus sulfur concentration for cement V with a w:c ratio of 0.4 is shown in Fig. 3.

The calcium and sulfur data for all the experimental conditions can be represented by the straight-line fits in Fig. 4, which show that the intensity of mixing did not seem to influence the ratio of calcium to sulfur for a particular cement paste. The

Ca:S ratio of the precipitating material, estimated from the changes in the calcium and sulfur concentrations, is between 0.4 and 1. The type of cement and the w:c ratio did influence the data, causing the trend lines in Fig. 4 to be displaced from each other.

Figure 5 shows the straight-line fits for the aluminum-versus-sulfur data, which have similar displacements for the different cement types and w:c ratios. However, the fits for the aluminum-versus-calcium data all fall on the same trend line, as shown in Fig. 6. The displacements in the calcium-versus-sulfur trend lines can be explained by the common-ion effect. Alkalis in the cement, which are generally present in the form of highly soluble compounds, cause the concentration of cations such as calcium to decrease; however, the alkalis do not directly affect the concentration of sulfur, which is present as  $\text{SO}_4^{2-}$ . There are ~50% more alkalis per unit weight in cement C than in cement V (0.49 wt% for cement C versus 0.33 wt% for cement V), so sodium and potassium in the aqueous phase of cement C have correspondingly higher concentrations. This condition causes the calcium concentrations to be lower with cement C. Similarly, at lower w:c ratios, the concentration of alkalis for a given cement are higher, causing the calcium concentrations to be lower.

Because aluminum exists in alkaline mediums as  $\text{Al}(\text{OH})_4^-$  rather than as a cation, the common-ion effect would not cause the observed effect. The cause of the displacements in the aluminum-versus-sulfur trend lines, as well as the apparent correlation between the aluminum and calcium concentrations, is unknown.

The type of mixing did influence the absolute concentrations (as opposed to the ratios) of calcium, sulfur, and aluminum in solution immediately after mixing (Stage 1) for a given cement type and w:c ratio. This phenomenon was particularly true at w:c = 0.4 (see Fig. 2 and Table III). Greater mixing energy (1 min of high-shear mixing) or longer mixing time (3 min of low-shear mixing) generally increased these concentrations. Note that there are no open symbols (low-energy mixing) with high concentrations of calcium and sulfur in Fig. 2. This observation indicates that the kinetics of mixing have a role in the absolute concentrations, but only for the first few minutes after combining cement and water.

As shown in Figs. 5 and 6, the Al:S and Al:Ca ratios are both ~1/400. If AFt is the early product, then at least some of the calcium (when Ca:S < 2) and virtually all of the aqueous aluminum combine to form product almost immediately as components dissolve from the reacting phases. The rapid reduction of ionic concentrations during this first 10-min period suggests that products precipitate rapidly and that the system is far from equilibrium. Another possible explanation for the decrease in calcium and sulfur over the first 10 min is the precipitation of gypsum from the aqueous phase. This belief assumes that the system is initially saturated with respect to calcium sulfate hemihydrate, which is reasonable. Unfortunately, this phase has not been included in our calculations. However, this does not explain the apparently proportional decline in aluminum concentration. At this point, the mechanism or mechanisms driving the decrease in concentrations is unclear.

(C) *Stage 3 (The Induction Period): Discussion of Fitting Experimental Data to Equilibria from the Computer Model:* Tables IV and V list the elemental concentrations as a function of time for the experiments performed up to 2 h after initial mixing. The alkali concentrations are approximately constant with time and are independent of the mixing condition; therefore, the values have been averaged into four conditions related to cement type and w:c ratio (see Table VI). All the invariant points in the  $\text{CaO-Al}_2\text{O}_3\text{-CaSO}_4\text{-H}_2\text{O}$  system were then calculated using these alkali concentrations. Both reported values for the solubility of  $\text{C}_3\text{AH}_6$  were used, which resulted in two slightly different sets of invariant points. One of these data sets predicted that monosulphoaluminate is not a stable phase, and the other set, using the preferred value for  $\text{C}_3\text{AH}_6$  solubility of Atkins *et al.*,<sup>17,27</sup> predicted that it was.

**Table IV. Elemental Concentrations for Various Mixing Procedures<sup>†</sup> Involving Cement Paste V**

Time <sup>‡</sup> (min)	Concentration					
	[Na] (mM)	[K] (mM)	[S] (mM)	[Ca] (mM)	[Al] (μM)	[Si] (μM)
	Mix design A					
1	5.57	68.63	51.37	40.64	110.55	35.75
16	6.79	71.47	25.69	24.75	88.00	46.20
61	7.22	75.27	23.54	26.12	95.15	28.60
91	7.21	73.00	23.26	26.34	90.75	48.95
121	8.18	80.59	26.62	27.94	96.80	40.15
	Mix design B					
1	3.16	41.07	45.71	55.44	130.35	22.00
16	3.81	44.09	18.42	30.74	99.55	48.95
31	3.89	44.99	17.66	35.42	106.70	28.05
61	3.89	44.01	16.34	37.02	111.10	40.15
91	3.79	42.86	15.95	37.18	107.80	37.95
121	4.15	45.64	17.22	36.96	108.35	42.90
	Mix design C					
5	7.05	78.05	30.80	26.07	91.30	60.50
20	7.22	76.03	24.97	24.58	88.00	39.05
35	6.88	72.76	23.16	26.90	90.75	47.85
65	7.61	76.05	22.66	32.29	100.10	41.25
95	7.61	76.05	22.22	29.43	95.15	48.40
125	7.49	74.71	22.27	29.81	101.75	50.60
	Mix design D					
5	5.07	52.05	33.06	36.74	110.00	36.85
20	4.28	46.25	18.43	26.79	94.05	44.00
35	4.77	50.34	18.98	30.69	101.75	35.75
65	4.74	49.03	17.22	34.49	107.80	36.85
95	5.03	50.48	18.70	33.11	105.60	30.80
125	4.98	49.99	17.44	31.46	102.30	40.15

<sup>†</sup>Mix designs "A"–"D" are described as follows: A—high-energy mixer, w:c = 0.4, mix time of 1 min; B—high-energy mixer, w:c = 0.7, mix time of 1 min; C—Hobart mixer, w:c = 0.4, mix time of 5 min; and D—Hobart mixer, w:c = 0.7, mix time of 5 min.

<sup>‡</sup>"Time" refers to the number of minutes after the water and cement are first mixed.

**Table V. Elemental Concentrations for Various Mixing Procedures<sup>†</sup> Involving Cement Paste C**

Time <sup>‡</sup> (min)	Concentration					
	[Na] (mM)	[K] (mM)	[S] (mM)	[Ca] (mM)	[Al] (μM)	[Si] (μM)
	Mix design E					
5	34.47	144.56	59.84	16.83	75.90	77.00
20	33.15	137.07	55.50	16.23	75.35	64.90
35	33.41	141.60	50.55	17.93	93.50	55.00
65	31.76	131.11	44.22	17.38	78.65	57.20
125	33.83	138.25	47.63	18.48	83.60	56.65
	Mix design F					
5	33.59	130.23	65.51	17.71	80.30	92.40
20	31.54	124.90	56.49	17.33	75.35	67.10
35	35.47	136.10	58.63	19.25	79.20	61.60
65	34.70	131.41	52.47	20.52	83.05	44.00
95	34.01	126.97	50.27	19.42	78.10	46.20
125	33.44	129.11	51.15	18.92	80.85	57.75
	Mix design G					
5	18.95	96.49	43.12	20.84	91.30	112.20
20	20.08	100.19	36.68	21.40	86.35	59.40
35	20.05	97.96	34.16	21.84	101.20	106.70
65	19.92	96.92	31.24	23.10	94.60	53.53
95	19.77	95.05	28.98	21.12	85.80	56.65
125	20.75	99.64	30.47	21.18	90.75	75.90
	Mix design H					
5	19.88	96.41	35.26	18.10	77.00	54.45
20	19.95	96.19	34.04	20.18	81.95	47.30
35	20.21	95.49	32.72	21.78	85.80	47.30
65	20.24	92.71	29.48	22.88	89.10	41.80
95	20.19	94.70	30.03	22.77	88.55	46.75
125	19.91	92.95	28.88	22.05	86.90	45.65

<sup>†</sup>Mix designs "E"–"H" are described as follows: E—high-energy mixer, w:c = 0.4, mix time of 5 min; F—Hobart mixer, w:c = 0.4, mix time of 5 min; G—high-energy mixer, w:c = 0.7, mix time of 5 min; and H—Hobart mixer, w:c = 0.7, mix time of 5 min.

<sup>‡</sup>"Time" refers to the number of minutes after the water and cement are first mixed.

**Table VI. Experimental Alkali Concentrations Used in the Model**

Cement <sup>†</sup>	Concentration (mM)	
	Potassium	Sodium
V (0.7)	45	4
V (0.4)	75	7
C (0.7)	96	20
C (0.4)	135	33

<sup>†</sup>The value given in parentheses is the ratio of water to cement (w:c).

Other differences included the appearance of phase assemblages in addition to those calculated by Damidot and Glasser.<sup>1,2</sup>

Damidot and Glasser<sup>2</sup> noted that the presence of potassium concentrations of >395 mM lead to the formation of syngenite, a salt with the formula  $\text{CaK}_2(\text{SO}_4)_2 \cdot \text{H}_2\text{O}$ ; syngenite does not have a corresponding sodium salt. None of the concentrations of potassium from this work were above this level; therefore, the formation of syngenite was not predicted. The mineral pentasalt,  $(\text{CaSO}_4)_5 \cdot \text{K}_2\text{SO}_4 \cdot \text{H}_2\text{O}$ , although not predicted by Damidot and Glasser<sup>2</sup> to be stable until above 40°C, was calculated to be stable under these experimental solution compositions. Pentasalt was removed as a possible stable phase because it has not been documented to be a major phase in cement pastes.

The first experimental data point plotted in Figs. 4 and 5 for Stage 1 (<1 min after mixing cement and water) and the data point for Stage 3 (2 h old, Tables IV and V) were compared with the calculated invariant points. The closest matching phase assemblages are listed in Table VII. The choice of the value for the equilibrium constant of  $\text{C}_3\text{AH}_6$  does not affect these results, because solution compositions in equilibrium with this phase are not close to those experimentally determined for cement. Comparison of the experimental values with the calculated invariant points makes several points clear. First and foremost, the invariant points are greatly affected by the concentration of alkalis. If alkalis are taken into account, the model correctly predicts the sulfur concentration at both Stage 1 and Stage 3 and the calcium concentration at Stage 3. Furthermore, the inclusion of alkalis is the only way to account for the high concentration of sulfur in the aqueous phase, which explains the difficulty of using Brown's<sup>14</sup> phase diagrams to interpret pore solution data of portland cements.

The solid phase assemblage most closely matching the experimental data of Stage 1 is the equilibrium between gypsum,  $\text{AH}_3$ , and ettringite, labeled as point E2 on the phase diagrams (see Fig. 1). The solid phase assemblage that most closely matches the Stage 3 data is an equilibrium between gypsum,

CH, and ettringite, which is similarly labeled point F. The concentrations of sulfur are predicted quite well for both times. The Stage 1 calcium concentration is predicted within an order of magnitude, and the Stage 3 calcium concentrations are predicted quite closely.

The predicted early concentration of aluminum is incorrect by one order of magnitude, and in Stage 3 it is several orders of magnitude too low. This problem was also observed by Damidot and Glasser<sup>1</sup> when they were comparing their predicted values for invariant points E2 and F to the experimental values for these phase assemblages reported by Jones<sup>10</sup> and D'Ans and Eick<sup>13</sup> for the system with no alkalis (see Table VIII).

The most likely explanation for the difference in aluminum concentration relating to point E2 is related to the form of  $\text{AH}_3$  assumed to be present, as noted by Damidot and Glasser.<sup>1</sup> The database used in this work and by Damidot and Glasser contains the solubility data for gibbsite ( $\gamma\text{-AH}_3$ ), which is the least-soluble polymorph. Jones<sup>10</sup> used a more-soluble crystalline form of  $\text{AH}_3$  (bayerite), while D'Ans and Eick<sup>13</sup> used both crystalline and gel forms of  $\text{AH}_3$ . A change in the solubility of  $\text{AH}_3$  could easily explain the order-of-magnitude difference in aluminum concentrations for point E2, and it is likely that the  $\text{AH}_3$  that precipitates in cement systems will initially be in a less-crystalline, more-soluble form. It is worth noting that the experimentally observed concentrations for Stage 1 from this work are in good agreement with the experimentally determined values for point E2, shown in Table VIII, when the presumed increase in aluminum concentration due to alkalis is taken into account.

Another possibility for the higher experimental aluminum concentrations is the formation of an amorphous material on the surface of the cement particles soon after mixing, which has been noted by several researchers and discussed by Scrivener.<sup>9</sup> This gelatinous layer most likely consists primarily of alumina and silica, as well as calcium and sulfate; this layer has a variable composition<sup>9</sup> and is likely to have a high solubility.

The very large difference between the predicted and experimental values of the aluminum concentration for point F is more difficult to explain. Clearly, either there is a problem with the model (or model database) or there is another phase relationship in effect. As with point E2, the experimentally observed aluminum concentrations for Stage 3 are in good agreement with the reported experimental values Jones<sup>10</sup> and D'Ans and Eick<sup>13</sup> used to define point F, when the effect of alkalis is taken into account (see Tables VII and VIII), which leads us to conclude that the discrepancy in the aluminum concentrations is associated with the model.

By including alkalis in the prediction of equilibria with solid

**Table VII. Comparison of Experimental Data to Model Calculations at Stages 1 and 3**

Cement type <sup>†</sup>	Concentration (mM)		Concentration (mM)	
	Experimental (stage 1)	Calculated (point E2)	Experimental (stage 3)	Calculated (point F)
	Calcium			
V (0.7)	58	11	32	23
V (0.4)	44	10	29	20
C (0.7)	40	10	22	18
C (0.4)	30	9	20	16
	Aluminum			
V (0.7)	0.15	0.011	0.10	$2.00 \times 10^{-7}$
V (0.4)	0.13	0.013	0.095	$2.00 \times 10^{-7}$
C (0.7)	0.13	0.014	0.09	$3.00 \times 10^{-7}$
C (0.4)	0.11	0.016	0.085	$3.00 \times 10^{-7}$
	Sulfur			
V (0.7)	54	35	20	21
V (0.4)	55	51	25	30
C (0.7)	65	67	32	40
C (0.4)	80	93	53	58

<sup>†</sup>The value given in parentheses is the ratio of water to cement (w:c).



**Table VIII. Calculated and Experimental Aluminum Concentrations for Invariant Points E2 (Gypsum,  $\text{Al}_2\text{O}_3 \cdot 3\text{H}_2\text{O}$ , and Ettringite) and F (Gypsum, Calcium Hydroxide, and Ettringite) for the  $\text{CaO}-\text{Al}_2\text{O}_3-\text{CaSO}_4-\text{H}_2\text{O}$  System with No Alkalis<sup>†</sup>**

Source	Aluminum concentration, [Al] (mM)	
	Point E2	Point F
Calculated (from Damidot and Glasser <sup>1</sup> )	0.001	0.0003
Experimental (from Jones <sup>10</sup> )	0.025	0.06
Experimental (from D'Ans and Eick <sup>13</sup> )	0.09	0.027

<sup>†</sup>After Damidot and Blasser.<sup>1</sup> Concentrations have been taken from Refs. 1, 10, and 13.

phases in the subsystem of  $\text{CaO}-\text{Al}_2\text{O}_3-\text{CaSO}_4-\text{H}_2\text{O}$ , compositions seem to move from a phase assemblage of gypsum,  $\text{AH}_3$ , and ettringite to an assemblage of gypsum, CH, and ettringite when cement paste ages from Stage 1 to Stage 3 (the induction period). Apparently, CH is present during the induction period.

#### (2) Silicates: The $\text{CaO}-\text{SiO}_2-\text{H}_2\text{O}$ System

The silicon concentrations were also measured for all the pastes, at reaction times ranging from 2 min to 2 h. Figures 7

and 8 show the silicon concentration plotted against the calcium concentration for the pastes made with cements V and C at a w:c ratio of 0.4. Solid symbols correspond to pastes made with the high-shear mixer, and open symbols correspond to those made with the Hobart mixer. Curves M and S are the respective metastable and stable solubility lines for the C-S-H gel phase, as described by Jennings.<sup>3</sup>

The calcium levels are highest immediately after mixing. More-energetic or longer mixing results in more calcium in solution at the end of Stage 1. The calcium concentration decreases rapidly during the first few minutes of reaction while the silicon concentration increases. This trend is represented by arrow "1" in Figs. 7 and 8. During the next 15 min or so, the calcium concentration increases again while the silicon concentration decreases, as shown by arrow "2." The primary difference between cements V and C is that the calcium concentration is higher in cement V. As discussed earlier, higher alkali concentrations in cement C pastes cause a greater depression of the calcium levels, as do lower w:c ratios, than for cement V.

#### IV. Summary

The effects of mixing intensity, the ratio of water to cement (w:c), and cement composition on the chemistry of the aqueous

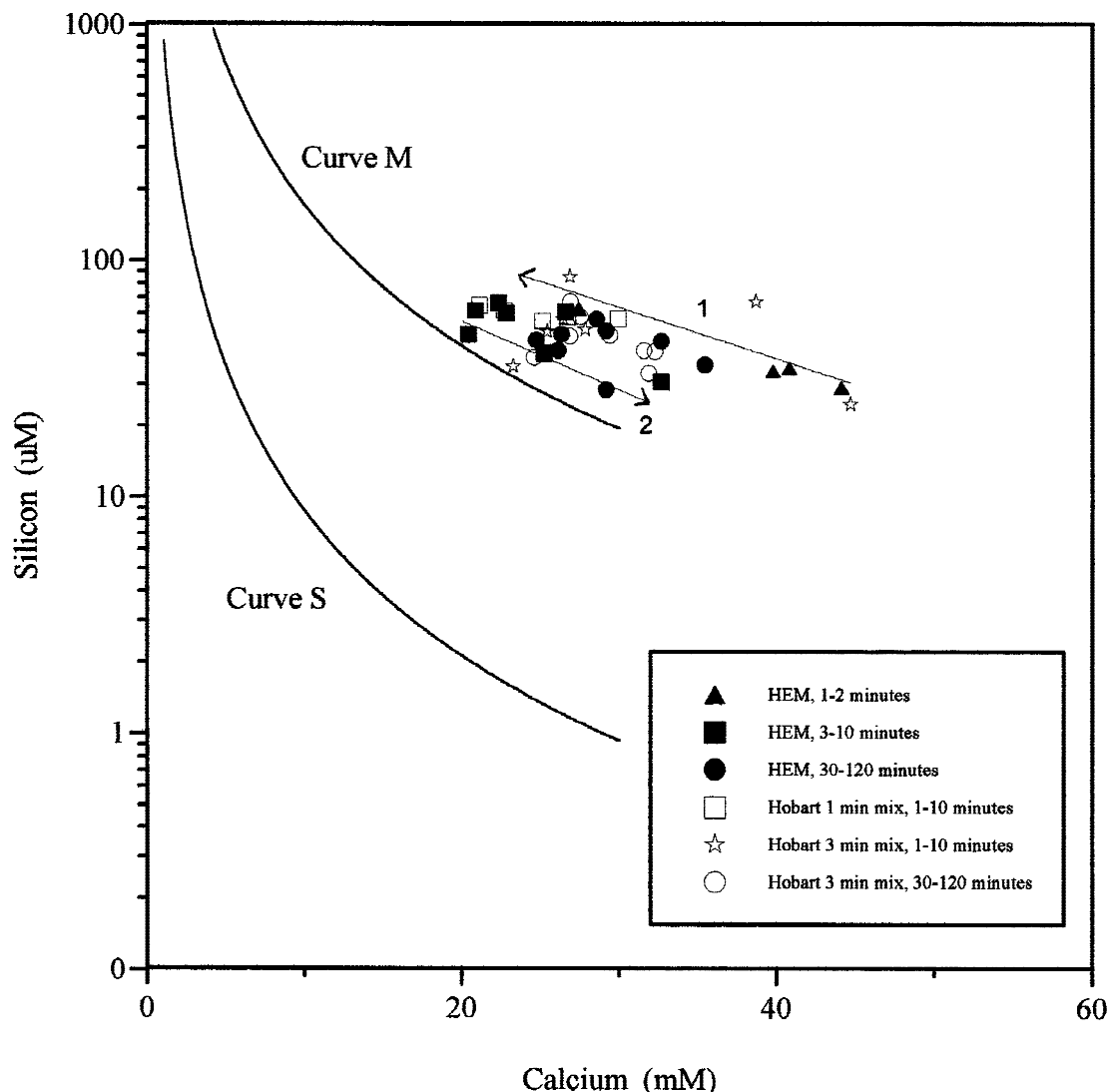


**Fig. 7.** Plot of silicon concentration versus calcium concentration for cement V pastes, at w:c = 0.4, for the first 2 h after mixing. Arrows indicate increasing time.

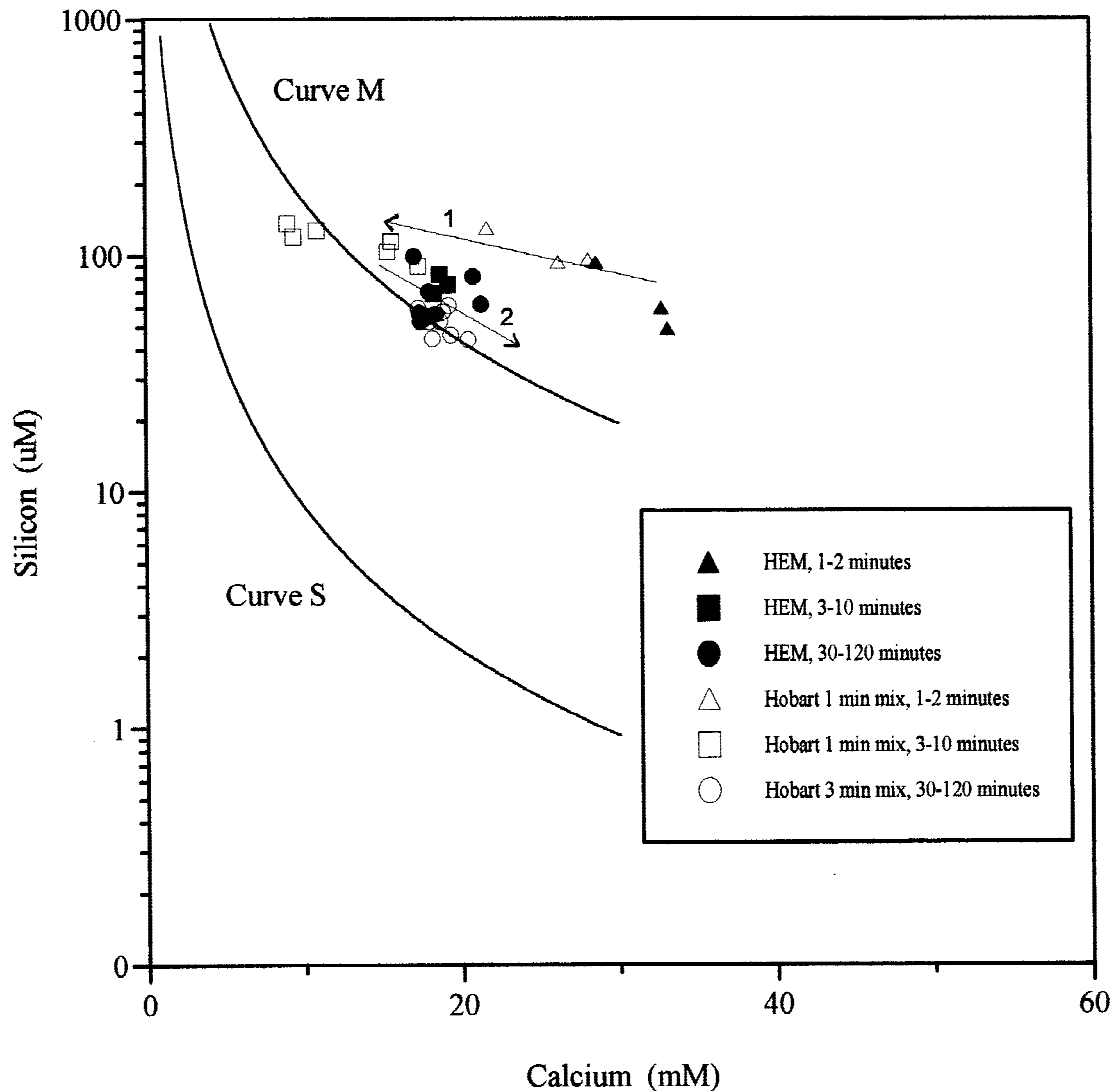


**Fig. 8.** Plot of silicon concentration versus calcium concentration for cement C pastes, at  $w:c = 0.4$ , for the first 2 h after mixing. Arrows indicate increasing time.

phase during the first few hours of the hydration of portland cement were investigated. The  $w:c$  ratio and the cement type affected the concentration of alkalis in the pore solution, which affected the concentrations of the other components throughout the first 2 h of reaction and beyond. The mixing intensity affected the concentrations of the ions during the first few minutes of reaction only, which strongly suggests that cement paste rapidly achieved a type of pseudo-equilibrium whereby the concentrations are controlled by the solubility products of solid phases rather than by the competing rates of dissolution and precipitation.

The analysis of the aqueous phase chemistry of the portland cement system was simplified by considering two subsystems: the  $\text{CaO-Al}_2\text{O}_3\text{-CaSO}_4\text{-H}_2\text{O}$  system (aluminates sulfates) and the  $\text{CaO-SiO}_2\text{-H}_2\text{O}$  system (silicates). Early hydration in the  $\text{CaO-CaSO}_4\text{-Al}_2\text{O}_3\text{-H}_2\text{O}$  system can be divided into three distinct stages: (i) rapid reaction of calcium and alkalis (<1 min after mixing); (ii) precipitation of aluminates during which concentrations of the major components (calcium, aluminum, and sulfur) decrease continuously (the first few minutes after the start of mixing); and (iii) quasi-equilibrium, during which the concentrations of the components remain relatively constant for up to 2 h. The relative concentrations of calcium, aluminum, and sulfur were constant for a given  $w:c$  ratio and cement type after the end of Stage 1. The cause of the decrease in concentrations during Stage 2, particularly the aluminum

concentration, is unclear. The behavior of the  $\text{CaO-SiO}_2\text{-H}_2\text{O}$  system was somewhat more complex; the silicon concentration increased slightly during the first few minutes and then decreased during Stage 2.

The experimental concentrations in the aluminate sulfate system at the end of Stage 1 and during Stage 3 were compared to predicted invariant points that represented various solid phase assemblages using the model and database developed by Damidot and Glasser.<sup>1,2</sup> From this analysis, it was concluded that the system moves from an equilibrium between gypsum,  $\text{AH}_3$ , and ettringite shortly after mixing to an equilibrium between gypsum, CH, and ettringite during the induction period. One problem with this analysis is the poor agreement between experimental and predicted aluminum concentrations for both phase assemblages. This variation, in the first case, is probably due to the use of data for the least-soluble form of  $\text{AH}_3$  (gibbsite) for the model, when a more-soluble form is likely to be present during early hydration. The cause of the discrepancy for the second invariant point is unknown. The experimental aluminum concentrations are in good agreement with experimentally determined values for these invariant points, as determined by other researchers in pure systems, which suggests that the problem lies with the model rather than with the interpretation.

**Acknowledgments:** The authors would like to acknowledge Prof. Fred

Glasser and Dr. Mark Atkins of Aberdeen University (Aberdeen, U.K.) for valuable discussions.

## References

- <sup>1</sup>D. Damidot and F. P. Glasser, "Thermodynamic Investigation of the CaO–Al<sub>2</sub>O<sub>3</sub>–CaSO<sub>4</sub>–H<sub>2</sub>O System at 25°C and the Influence of Na<sub>2</sub>O," *Cem. Concr. Res.*, **23**, 221–38 (1993).
- <sup>2</sup>D. Damidot and F. P. Glasser, "Thermodynamic Investigation of the CaO–Al<sub>2</sub>O<sub>3</sub>–CaSO<sub>4</sub>–K<sub>2</sub>O–H<sub>2</sub>O System at 25°C," *Cem. Concr. Res.*, **23**, 1195–204 (1993).
- <sup>3</sup>H. M. Jennings, "Aqueous Solubility Relationships for Two Types of Calcium Silicate Hydrate," *J. Am. Ceram. Soc.*, **69** [8] 614–18 (1986).
- <sup>4</sup>D. D. Double, "New Developments in Understanding the Chemistry of Cement Hydration," *Philos. Trans. R. Soc. London A*, **A310**, 53–66 (1983).
- <sup>5</sup>E. M. Gartner, F. J. Tang, and S. J. Weiss, "Saturation Factors for Calcium Hydroxide and Calcium Sulfates in Fresh Portland Cement Pastes," *J. Am. Ceram. Soc.*, **68** [12] 667–73 (1985).
- <sup>6</sup>C. D. Lawrence, "Changes in Composition of the Aqueous Phase During Hydration of Cement Pastes and Suspensions"; p. 378 in *Symposium on Structure of Portland Cement Paste and Concrete (Special Report 90)*. Highway Research Board, Washington, DC, 1966.
- <sup>7</sup>K. Matsukawa and S. Diamond, "Quantitative Study of Naphthalene Sulfonate Effects on Cement Paste Pore Solution Chemistry"; pp. 41–55 in *Ceramic Transactions, Vol. 16, Advances in Cementitious Materials*. Edited by S. Mindess. American Ceramic Society, Westerville, OH, 1991.
- <sup>8</sup>H. F. W. Taylor, *Cement Chemistry*. Academic Press, London, U.K., 1990.
- <sup>9</sup>K. L. Scrivener, "The Microstructure of Concrete"; pp. 127–61 in *Materials Science of Concrete I*. Edited by J. P. Skalny. American Ceramic Society, Westerville, OH, 1989.
- <sup>10</sup>F. E. Jones, "The Quaternary System CaO–Al<sub>2</sub>O<sub>3</sub>–CaSO<sub>4</sub>–H<sub>2</sub>O at 25°C," *J. Phys. Chem.*, **48**, 311–55 (1944).
- <sup>11</sup>F. E. Jones, "The Quinary System CaO–Al<sub>2</sub>O<sub>3</sub>–CaSO<sub>4</sub>–K<sub>2</sub>O–H<sub>2</sub>O (1 Per Cent K<sub>2</sub>O) at 25°C," *J. Phys. Chem.*, **48**, 356–78 (1944).
- <sup>12</sup>F. E. Jones, "The Quinary System CaO–Al<sub>2</sub>O<sub>3</sub>–CaSO<sub>4</sub>–Na<sub>2</sub>O–H<sub>2</sub>O (1 Per Cent Na<sub>2</sub>O) at 25°C," *J. Phys. Chem.*, **48**, 379–94 (1944).
- <sup>13</sup>J. D'Ans and H. Eick, "Das System CaO–Al<sub>2</sub>O<sub>3</sub>–CaSO<sub>4</sub>–H<sub>2</sub>O bei 20°C," *Zem.-Kalk-Gips*, **6**, 302 (1953).
- <sup>14</sup>P. W. Brown, "Phase Equilibria and Cement Hydration"; see Ref. 9, pp. 73–93.
- <sup>15</sup>D. L. Parkhurst, D. C. Thorstenson, L. N. Plummer, "PHREEQE Computer Program for Geochemical Calculations," Water Resources Investigations Rept. No. 80-96, U.S. Geological Survey, Denver, CO, 1980.
- <sup>16</sup>J. C. Westfall, J. L. Zachary, and F. M. Morel, "MINEQL—A Computer Program for the Calculation of Chemical Equilibrium Compositions of Aqueous Systems," Dept. of Civil Engineering, Massachusetts Institute of Technology, Cambridge, MA, 1976.
- <sup>17</sup>M. Atkins, D. Bennett, A. Dawes, F. Glasser, A. Kindess, and D. Read, "A Thermodynamic Model for Blended Cements," 1991 U.S. Dept. of Energy Report No. DOE/HMIP/PR/92/005.
- <sup>18</sup>E. P. Flint and L. S. Wells, "Study of the System CaO–SiO<sub>2</sub>–H<sub>2</sub>O at 30°C and the Reaction of Water on Anhydrous Calcium Silicates," *NBS J. Res.*, **12**, 751–83 (1934).
- <sup>19</sup>K. Fujii and W. Kondo, "Heterogeneous Equilibrium of Calcium Silicate Hydrate in Water at 30°C," *J. Chem. Soc., Dalton Trans.*, **2**, 645–51 (1981).
- <sup>20</sup>K. Fujii and W. Kondo, "Hydration of Tricalcium Silicate," *Proc. Int. Symp. Chem. Cem.*, **5th**, **2**, 362–71 (1968).
- <sup>21</sup>P. Fierens and J. P. Verhaegen, "Filter Dissolution of C<sub>3</sub>S as a Function of the Lime Concentration in a Limited Amount of Lime Water," *Cem. Concr. Res.*, **10**, 521 (1980).
- <sup>22</sup>N. L. Thomas and D. D. Double, "Calcium and Silicon Concentrations in Solution During the Early Hydration of Portland Cement and Tricalcium Silicate," *Cem. Concr. Res.*, **11**, 675 (1981).
- <sup>23</sup>P. W. Brown, E. Franz, G. Frohnsdorff, and H. F. W. Taylor, "Analyses of the Aqueous Phase During Early C<sub>3</sub>S Hydration," *Cem. Concr. Res.*, **14**, 257–62 (1984).
- <sup>24</sup>P. W. Brown, "The System Na<sub>2</sub>O–CaO–SiO<sub>2</sub>–H<sub>2</sub>O," *J. Am. Ceram. Soc.*, **73** [11] 3457–61 (1990).
- <sup>25</sup>P. W. Brown and D. Shi, "A Model for the Variations in Solution Chemistry During Tricalcium Silicate Hydration," *Adv. Cem. Res.*, **4** [1] 17–27 (1991).
- <sup>26</sup>S. K. Hodson, "Apparatus for Producing Cement Building Material," U.S. Pat. No. 4 944 595, July 31, 1990.
- <sup>27</sup>M. Atkins; personal communication. □